Cell Reports
Methods

Article

Rapid detection of multiple SARS-CoV-2 variants of concern by PAM-targeting mutations

Graphical abstract

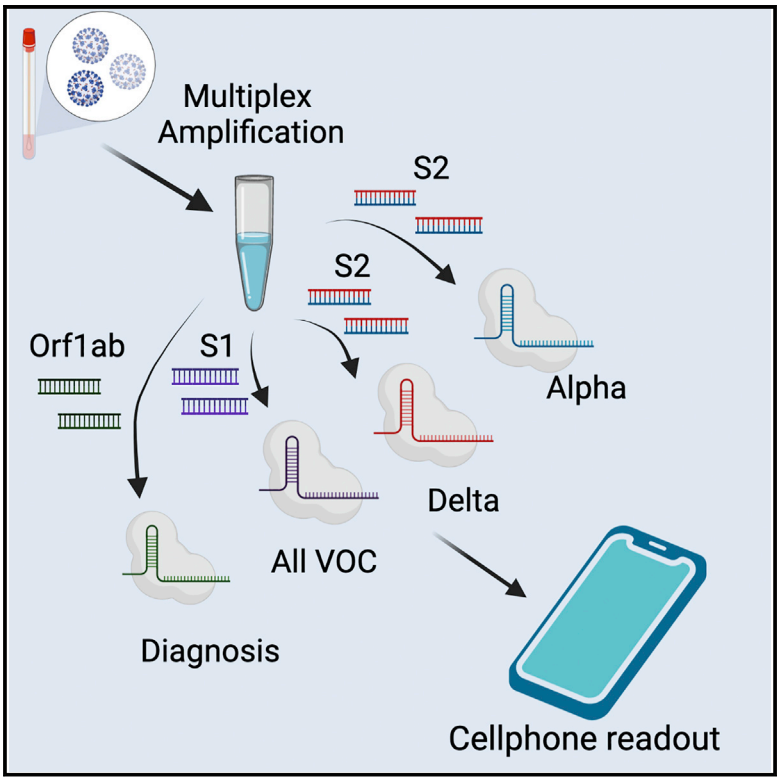

Authors

Bo Ning, Brady M. Youngquist, Diane D. Li, ..., Nicholas J. Maness, Di Tian, Tony Y. Hu

Correspondence

tonyhu@tulane.edu

In brief

Ning et al. report a CRISPR-Cas12a method that detects single-nucleotide polymorphisms (SNPs) in COVID-19 variants for rapid variant identification in patient samples. Using a quantitative smartphone readout, the method can detect multiple SNPs that affect CRISPR-Cas12a PAM and seed regions.

Highlights

- Smartphone diagnosis can distinguish SARS-CoV-2 variants in patient samples
- Single base-pair changes are detected with easy-to-integrate CRISPR-Cas12a test design
- Rapid SARS-CoV-2 variant detection compared with next-generation sequencing
- Approach can be adapted for specific detection of future SARS-CoV-2 variants

Ning et al., 2022, Cell Reports Methods 2, 100173
February 28, 2022
https://doi.org/10.1016/j.crmeth.2022.100173

CellPress

Cell Reports Methods

CellPress
OPEN ACCESS

Article

Rapid detection of multiple SARS-CoV-2 variants of concern by PAM-targeting mutations

Bo Ning,[1,2,6] Brady M. Youngquist,[1,2,6] Diane D. Li,[1,2] Christopher J. Lyon,[1,2] Adrian Zelazny,[3] Nicholas J. Maness,[4] Di Tian,[5] and Tony Y. Hu[1,2,7,*]

[1]Center for Cellular and Molecular Diagnostics, Tulane University School of Medicine, New Orleans, LA, USA
[2]Department of Biochemistry and Molecular Biology, Tulane University School of Medicine, New Orleans, LA, USA
[3]Department of Laboratory Medicine, Clinical Center, National Institutes of Health, Bethesda, MD, USA
[4]Tulane National Primate Research Center, Covington, LA, USA
[5]The Molecular Pathology Laboratory, Department of Pathology and Laboratory Medicine, Tulane University School of Medicine, New Orleans, LA, USA
[6]These authors contributed equally
[7]Lead contact
*Correspondence: tonyhu@tulane.edu
https://doi.org/10.1016/j.crmeth.2022.100173

MOTIVATION Fast and accurate detection of SARS-CoV-2 variants is necessary to track variant spread and understand their clinical phenotypes, which can affect COVID-19 diagnostic tests, treatment decisions, and vaccine effectiveness. Current SARS-CoV-2 variant detection workflows can be resource intensive and involve multiple steps. As such these approaches are sub-optimal for large-scale variant screening efforts needed during the pandemic, especially in resource-limited settings. Here, we describe a CRISPR-Cas12a assay designed to specifically detect SARS-CoV-2 variants in clinical samples during diagnosis. Our single-nucleotide polymorphism (SNP) detection design can potentially be used to track newly emerging SARS-CoV-2 variants.

SUMMARY

SARS-CoV-2 variants of concern (VOCs) that increase transmission or disease severity or reduce diagnostic or vaccine efficacy continue to emerge across the world. Current methods available to rapidly detect these can be resource intensive and thus sub-optimal for large-scale deployment needed during a pandemic response. Here, we describe a CRISPR-based assay that detects mutations in spike gene CRISPR PAM motif or seed regions to identify a pan-specific VOC single-nucleotide polymorphism (SNP)) ((D614G) and Alpha- and Delta-specific (S982A and D950N) SNPs. This assay exhibits good diagnostic sensitivity and strain specificity with nasal swabs and is designed for use in laboratory and point-of-care settings. This should enable rapid, high-throughput VOC identification required for surveillance and characterization efforts to inform clinical and public health decisions. Furthermore, the assay can be adapted to target similar SNPs associated with emerging SARS-CoV-2 VOCs, or other rapidly evolving viruses.

INTRODUCTION

New SARS-CoV-2 variants of interest (VOIs) and variants of concern (VOCs) continue to emerge worldwide, and while several have demonstrated the ability to rapidly displace the dominant strain(s) at their site of first detection and globally, relatively little is known about the clinical and epidemiologic characteristics until after they achieve local dominance due to limitations in currently available screening capacity. The ability to rapidly detect the emergence of newly identified variant strains has multiple important clinical implications, since new variants may affect symptom severity (Horby et al., 2021), mortality risk (Davies et al., 2021b), re-infection (Wibmer et al., 2021), and vaccine escape (Lopez Bernal et al., 2021) rates, and the response to specific monoclonal antibody treatments (Baum et al., 2020). For example, multiple studies have shown that mutations in SARS-CoV-2 VOCs (e.g., B.1.1.7 [Alpha], B.1.351 [Beta], P.1 [Gamma], and B.1.617.2 [Delta]) can reduce the therapeutic response to specific monoclonal antibodies and convalescent plasma used to attenuate COVID-19 severity (Li et al., 2020;

Liu et al., 2021; Wang et al., 2021a). Identification of the SARS-CoV-2 variants at diagnosis can thus provide actionable information that clinicians can use to select the most effective treatment. This is not currently feasible, however, since existing approaches used for strain-specific diagnosis approaches are inefficient, requiring multi-step variant detection strategies that cannot be applied to track variants at the population level in real time.

No COVID-19 diagnostic test currently available allows rapid, high-throughput detection of SARS-CoV-2 variants (Jayamohan et al., 2021). Next-generation sequencing (NGS) is the gold standard for variant identification but is expensive, low-throughput, and technically demanding, and cannot be used as a routine diagnostic test (Chiara et al., 2021). Reliance on NGS data for strain identification has delayed our understanding of the clinical phenotype of emerging variants, particularly during their early expansion when they may represent a relatively small fraction of the total cases, and there is a critical need for scalable COVID-19 diagnostic tests that can rapidly identify specific variants quickly to inform clinical decisions (Hafeez et al., 2021).

The utility of such tests was demonstrated during the emergence of the SARS-CoV-2 Alpha variant in the UK, where S-gene target failure (SGTF) in samples with positive signal for the SARS-CoV-2 nucleoprotein gene target was found to identify individuals infected with the Alpha variant (Brown et al., 2021; Davies et al., 2021a). SGTF in these assays was found to reflect a strain-specific deletion event in the Alpha variant and the SGTF rate of this dual assay was therefore used to robustly evaluate the clinical phenotype of the Alpha variant in multiple large studies that used sample sizes that would not have been feasible to achieve with NGS data (Challen et al., 2021a; Volz et al., 2021).

SGTF assays have limited utility for strain discrimination, however, since many variants lack strain-specific deletion events required for specific identification by these assays, and the vast majority of mutations in the SARS-CoV-2 genome are SNPs (Nagy et al., 2021). Rapid scalable tests capable of detecting current and future variants should thus be capable of accurately detecting strain-specific SNPs to differentiate variants lacking targetable deletion events. However, most current methods used to detect specific SNPs exhibit variable sensitivity or specificity or are not feasible for use in high-throughput clinical workflows required to screen for the prevalence of emerging VOC strains (Gravagnuolo et al., 2021).

CRISPR ribonucleoprotein complexes can detect SNPs with high specificity as directed by the sequence of their gRNAs (Chen et al., 2020b, 2021b; Huang et al., 2021a; Meng et al., 2021; Myhrvold et al., 2018). Multiple assays that use CRISPR to detect SARS-CoV-2 gene targets have received Emergency Use Authorization from the FDA for COVID-19 diagnosis (Huang et al., 2021b; Palaz et al., 2021) and a few have been adapted for point-of-care applications to permit SARS-CoV-2 diagnosis in resource-limited settings (Arizti-Sanz et al., 2020; Broughton et al., 2020; Joung et al., 2020; Ning et al., 2021; Ramachandran et al., 2020).

Given the sequence specificity of CRISPR, we evaluated the ability of a multi-target CRISPR-Cas12a assay to simultaneously diagnose SARS-CoV-2 infection and detect strain-specific SNPs in the SARS-CoV-2 genome for variant identification. Single-nucleotide mismatches between Cas12a gRNAs and their target DNAs often do not produce detectable difference in the non-specific secondary cleavage activity of CRISPR Cas12a complexes to allow the detection of such sequences by cleavage-induced activation of a quenched oligonucleotide probe. However, SNPs that alter consensus PAM sequence motifs in DNA targets recognized by Cas12a gRNAs can markedly reduce this activity, as can mismatch in a "seed" region spanning the adjacent six nucleotides immediately downstream of this motif. Several studies have employed CRISPR-Cas systems to detect SNPs, although each of these has limitations that could reduce their clinical utility. One study used differential Cas9 *cis*-cleavage activity at a mutant site to distinguish two Zika virus strains via the effect of template destruction on a toehold sensor in an assay requiring 3.5–4.5 h. This study did not perform a complete analytical or clinical validation to characterize assay performance, although it indicated that a viral load of 1.7×10^6 copies/mL was within its detection limit (Pardee et al., 2016). Another study evaluated the effect of CRISPR-Cas12b seed region mutations on *trans*-cleavage of a fluorescent probe, but did not study PAM-altering mutations and did not perform a clinical validation study to evaluate the feasibility of this approach for clinical diagnosis (Teng et al., 2019). A third study recently employed CRISPR Cas12a to detect SARS-CoV-2 and its SARS-CoV-2 E484K mutation using a duplex saliva assay read by a point-of-care device (de Puig et al., 2021). However, a limitation of this assay was that the E484K mutation analyzed is not completely strain specific (Jangra et al., 2021) and the authors did not evaluate the potential of this approach for specific identification of other PAM or seed sequence mutations specific for other SARS-CoV-2 VOCs. Here, we describe a CRISPR Cas12a method that detects common, strain-specific SARS-CoV-2 SNPs that affect Cas12a PAM or seed regions in most variants to allow rapid SARS-CoV-2 strain identification at diagnosis by direct analysis of standard clinical samples.

Studies presented in this manuscript indicate that major SARS-CoV-2 VOC strains contain mutations that alter several distinct PAM motifs or their seed regions located in the SARS-CoV-2 spike gene, and that CRISPR-based assays employing guide RNAs (gRNAs) specific for these altered sequences can identify individual VOC strains with good diagnostic sensitivity and specificity. These VOC-specific CRISPR assays are suitable for high-throughput use in standard clinical laboratories and in a point-of-care assay read by a smartphone device, and thus have the potential to greatly expand the screening capacity for SARS-CoV-2 VOC strains to improve the tracking of emerging VOCs and understanding of their distinct clinical properties.

RESULTS

Optimization of CRISPR-based fluorescent detection system of genomic RNA from different SARS-CoV-2 variants

Since late December 2020, sequencing efforts have identified multiple SARS-CoV-2 VOIs or VOCs containing SNPs) or other mutations that alter the amino acid sequence of the SARS-CoV-2 Spike (S) protein from that of the USA-WA1/2020 CDC reference isolate (WA1) first detected the US in January 2020.

Table 1. CRISPR-Cas12a PAM sequence counts in SARS-CoV-2 spike genome

Strains	PAM	uPAM	Seed	uSeed	Other	uOther	Del	uDel	uPAM/seed (%)
Alpha	1	1	2	1	6	4	1	1	66.7
Beta	1	0	4	3	3	2	0	0	60.0
Gamma	4	4	3	2	3	3	0	0	85.7
Delta	4	3	3	2	4	3	0	0	71.4

uPAM, unique PAM sequences; uSeed, unique seed region; uOther, unique other sequence; Del, deleted sequences. uDel, unique deleted sequences.

This includes a D614G substitution that is consistently found in all major VOCs (Hou et al., 2020; Korber et al., 2020; Plante et al., 2021).

Sequence analysis of the spike gene of each of the four major VOC strains (Alpha, Beta, Gamma, and Delta) detected 8 to 11 mutated sites per strain versus the reference WA1 isolate, and 5 to 9 of these sites (63%–90%) were strain specific. The majority (90%; 27 of 30) of these sites represented SNPs, and many of these overall mutations (33%–70%) altered candidate PAM motifs or their adjacent seed regions, with most (60%–86%) demonstrating strain specificity, so that each strain had 2 to 5 strain-specific PAM motif or seed region mutations (Table 1; Figure S1A). Notably, these strain-specific PAM and seed region mutations comprised the majority (60%–67%) of all strain-specific mutations in three of the four VOC strains a lesser fraction (33%) of these sites in the remaining VOC strain.

Mutations that affected PAMs or their seed sequences appeared to be somewhat uniformly distributed in the spike gene, and their resulting amino changes were distributed across most of the spike protein surface area (Figure 1A). However, multiple strain-specific PAM and seed motif mutations, and a PAM mutation pan-specific for all VOC strains, were found to cluster in two short (<500 nucleotide) RNA sequence regions encoding the S1 receptor binding domain and its C-terminal region and the second hinge region of the S2 domain (Figure 1B)

To permit rapid, sensitive, and high-throughput detection of SARS-CoV-2 variants in clinical samples analyzed in resource-limited settings we employed a CRISPR-Cas12a-based isothermal amplification assay we recently developed for SARS-CoV-2 diagnosis (Huang et al., 2020). We have previously employed a variation of this method to permit RNA isolation-free detection of SARS-CoV-2 in saliva (Ning et al., 2021). However, we did not employ this approach in this study since this would have required prospective sample collection and limited the strains available for analysis due to the limited strain diversity nationwide at study performance. We instead chose to analyze RNA extracted from standard nasal swab samples to permit greater strain coverage. Multiplex RT-PCR (80 min) or RT-RPA (reverse transcription-recombinase polymerase amplification) (15 min) reactions (20 μL) were employed to amplify an Orf1ab gene target sequence to permit general SARS-CoV-2 diagnosis, and two spike gene amplicons containing three strain-specific SNPs of interest. Following amplification, multiplex PCR reaction aliquots were added to four separate CRISPR-Cas12a cleavage reactions with target-specific guide RNAs, and Cas12a *trans*-cleavage of a quenched fluorescent reporter oligonucleotide induced in proportion to the target sequence was quantified by a microplate reader or smartphone readout device (15 min).

We hypothesized that CRISPR fluorescence detection system (FDS) assays employing gRNAs targeting altered PAM motifs, and potentially other strain-specific mutations, could distinguish VOC strains with high specificity (Figure S1B). To test this hypothesis, we identified primer pairs that spanned three regions of the SARS-CoV-2 genome to generate amplicons that contain a conserved Orf1ab target, an S1 region encompassing the pan-specific VOC D614G, SNP sites, and an S2 region containing the Delta-specific D950N and Alpha-specific S982A SNP sites (Figure 1B; Table S1). We selected the D950N and S982A mutations for our multiplex assay to reflect strain prevalence and clinical availability at study performance. Multiplex CRISPR-FDS assays that detected the ORF1ab site, and D614G, D950N, and S982A sites that created (D950N; positive signal) or disrupted (S982A; loss of signal) consensus PAM sites or altered their seed sequences (D614G; positive signal), respectively, detected all strains, all VOC strains, and the Delta and Alpha strains (Figure 1C). Subsequent optimization for multiplex amplification of the three target amplicons (Orf1ab, S1, and S2) revealed that a narrow annealing temperature range was required for efficient multiplex PCR amplification, that optimal signal in a subsequent D950N-specific CRISPR-FDS assay was detected at 42°C (Figure 1D), and that the signal-to-noise ratio of this assay increased in proportion to probe and Cas12a/gRNA complex concentration (Figures 1E–1G), with similar results detected for D614G- and S982A-specific CRISPR-FDS assays (Figure S2). To determine the ability of this approach to detect target RNA in samples without RNA isolation, viral seed stock aliquots from VOC strains were mixed and incubated with lysis buffer and then directly employed as the assay input samples (Figure 1H).

Analytical validation of CRISPR-FDS assays detecting different SARS-CoV-2 strains

SNP-specific CRISPR readout assays for multiplex RT-PCR were subjected to analytical validation studies using genomic RNA isolated from *in vitro* cultures of sequence-confirmed SARS-CoV-2 isolates obtained from clinical samples, including all VOC strains (Table S2). Consistent with expected results, all SARS-CoV-2 and all VOC samples exhibited similar signals for ORF1ab and D614G, respectively (Figures 2A and 2B), while SNPs that created and destroyed a D950N and S982A SNP were detected only in the Delta and Alpha samples by the gain (D950N) and loss (S982A) of CRISPR signal (Figures 2C and 2D). The Beta-specific SNP D80A also caused a seed region mutation that distinguished it from all other VOC strains, but was not pursued due to our inability to obtain clinical samples confirmed to contain the Beta VOC strain (Figure S3). Since the S982A assay resulted in the loss of CRISPR signal,

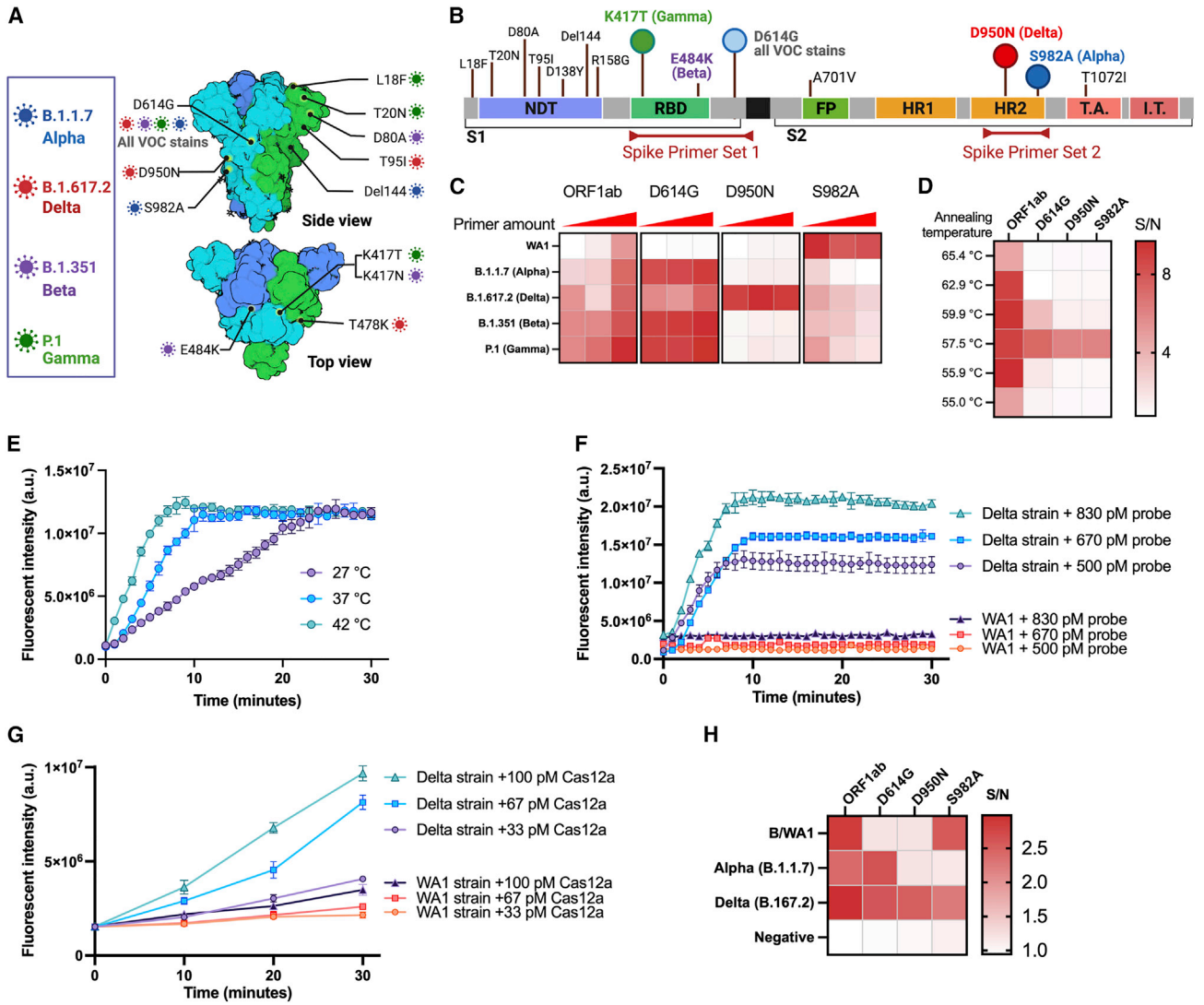

Figure 1. CRISPR-mediated detection of selected SARS-CoV-2 variants

(A) Rendering of the SARS-CoV-2 spike protein trimer (https://www.rcsb.org, PDB: 6VXX) indicating the position of key mutations associated with specific SARS-CoV-2 VOCs, with boxes indicating VOC-specific mutations.

(B) Map of mutation sites relative to known functional domains in SARS-CoV-2 spike protein sequence, with key mutations and amplicons that contain them denoted by colored symbols and text and underlined regions.

(C and D) Optimization of (C) RT-RPA multiplex detection and (D) primer annealing temperature in a multiplex RT-PCR reaction using 1 μg genomic RNA samples from (C) the indicated SARS-CoV-2 strains or (D) B.1.617.2, as evaluated by CRISPR-FDS signal-to-noise ratios when 2 μL of RT-RPA or RT-PCR product was incubated at 37°C for 15 min with 30 μL of CRISPR reagents. Signal-to-noise is defined as the ratio of fluorescent signal for a sample well versus the mean fluorescence detected in its matching no template control (NTC) wells.

(E–G) CRISPR-FDS signal from CRISPR-FDS reactions using varying (E) temperatures, (F) D950N probe, and (G) Cas12a protein concentrations upon analysis of 2 μL of 20 μL RT-PCR reactions containing 1 μg genomic RNA of the WA1 (C–E) and B.1.617.2 (D and E) strains. Graphs indicate the mean ± SD of triplicate samples.

(H) RNA isolation-free detection of VOC strains: 5 μL of 10^3 TCID50/μL of the indicated SARS-CoV-2 strains was evaluated by isolation-free CRISPR-FDS signal-to-noise ratios.

samples had to have positive ORF1ab signal and negative S982A signal to be identified as Alpha variant positive. D614G, D950N, and S982A signals detected in standard curves generated with RNA extracted from healthy nasal swab replicates spiked with dilutions of genomic RNA from SARS-CoV-2 Gamma and WA1 isolates robustly differentiated the blank and lowest concentration standard (0.5 copies/μL) for all three assays (Figures 2E–2G) and revealed strong linearity and correlation (R^2 = 0.88 to 0.94) across the dilution range (0.5–1,000 copies/μL; Figures 2H–2J).

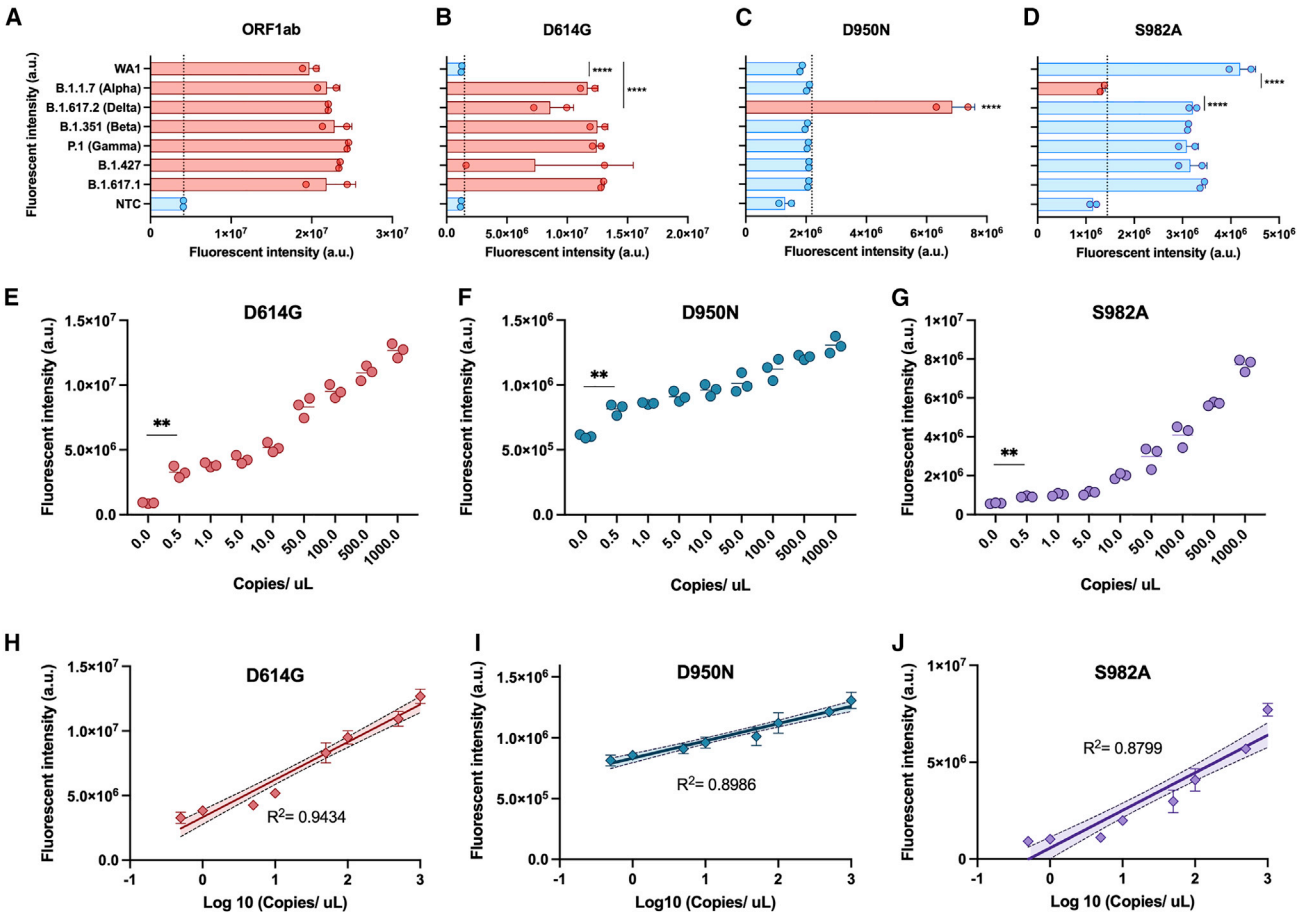

Figure 2. Analytical validation of CRISPR-FDS assay sequence specificity

(A–D) Signal produced by CRISPR-FDS assays that target (A) an ORF1ab sequence, and S protein sites that can contain (B) D614G, (C) D950N, and (D) S982A mutations in the indicated SARS-CoV-2 strains and a no template control (NTC). Positive CRISPR signal thresholds were defined as the mean plus three times the SD of the NTC, with positive and negative results marked in red and blue, respectively.

(E–G) Limit of detection (LoD) assays for (E) D614G, (F) D950N, and (G) S982A indicating an LoD of 0.5 copies/μL for each target. LoD was performed using serially diluted viral RNA of known concentration in healthy nasal swab samples.

(H–J) Standard curves of CRISPR-FDS assays employing gRNAs targeting the (H) D614G, (I) D950N, and (J) S982A mutants (50–100,000 copies genomic RNA of SARS-CoV-2 Delta strain). Cas12a incubation time was standardized at 15 min. Graphs indicate the mean ± SD of triplicate samples. Standard curve graphs depict the linear regression line of the data, its 95% CI, and Pearson correlation coefficient. **p < 0.01, ****p < 0.0001 by two-way ANOVA test.

Evaluation of the diagnostic performance of CRISPR-FDS assays with differential specificity

Minimum thresholds for positive signal were next determined using receiver operator characteristic curve cut points to distinguish signal from nasal swab RNA isolates of individuals with sequence-confirmed infections caused by SARS-CoV-2 strains that do and do not contain the targeted SNP sequence (Figures 3A–3C; Table S3). CRISPR-FDS assays using these signal thresholds were then applied to CRISPR-FDS assays that analyze nasal swab samples from 12 uninfected individuals and 71 individuals with SARS-CoV-2 infections (16 Alpha, 44 Delta, and 10 WA1/B strains) (Table S4). These assays demonstrated high diagnostic sensitivity and specificity for specific detection of all SARS-CoV-2 infections (ORF1ab positive; 98.5% and 100%) the detection of VOC (D614G positive; 86.7% and 95.5%), SARS-CoV-2 Delta (D950N positive; 97.6% and 94.8%), and Alpha (S982A negative; 88.2% and 92.6%) cases among infected individuals (Figure 3D). CRISPR signal detected in patients with confirmed Delta isolates was greater than the signal detected in patients with Alpha or B/WA1 isolates (Figure 3E). The signal for the VOC pan-specific D614G SNP was also greater in samples from patients with sequence-confirmed Delta versus Alpha SARS-CoV-2 isolates, apparently reflecting the greater viral load in the Delta samples (Figure 3F). A similar effect was observed for S982A where the signal indicating the absence of this SNP was stronger in Delta versus B/WA1 isolates (Figure 3H), while a Delta-specific D950N signal was detected almost exclusively in Delta isolates with a signal intensity range similar to that observed for other SNP markers in this sample group (Figure 3G). CRISPR ORF1ab signal exhibited a strong-negative correlation (Pearson $r = -0.68$) with qRT-PCR assay Ct values (Figure 3I), supporting the quantitative nature of these results in clinical samples (Figure S4). Notably, Delta cases were responsible for most (63%)

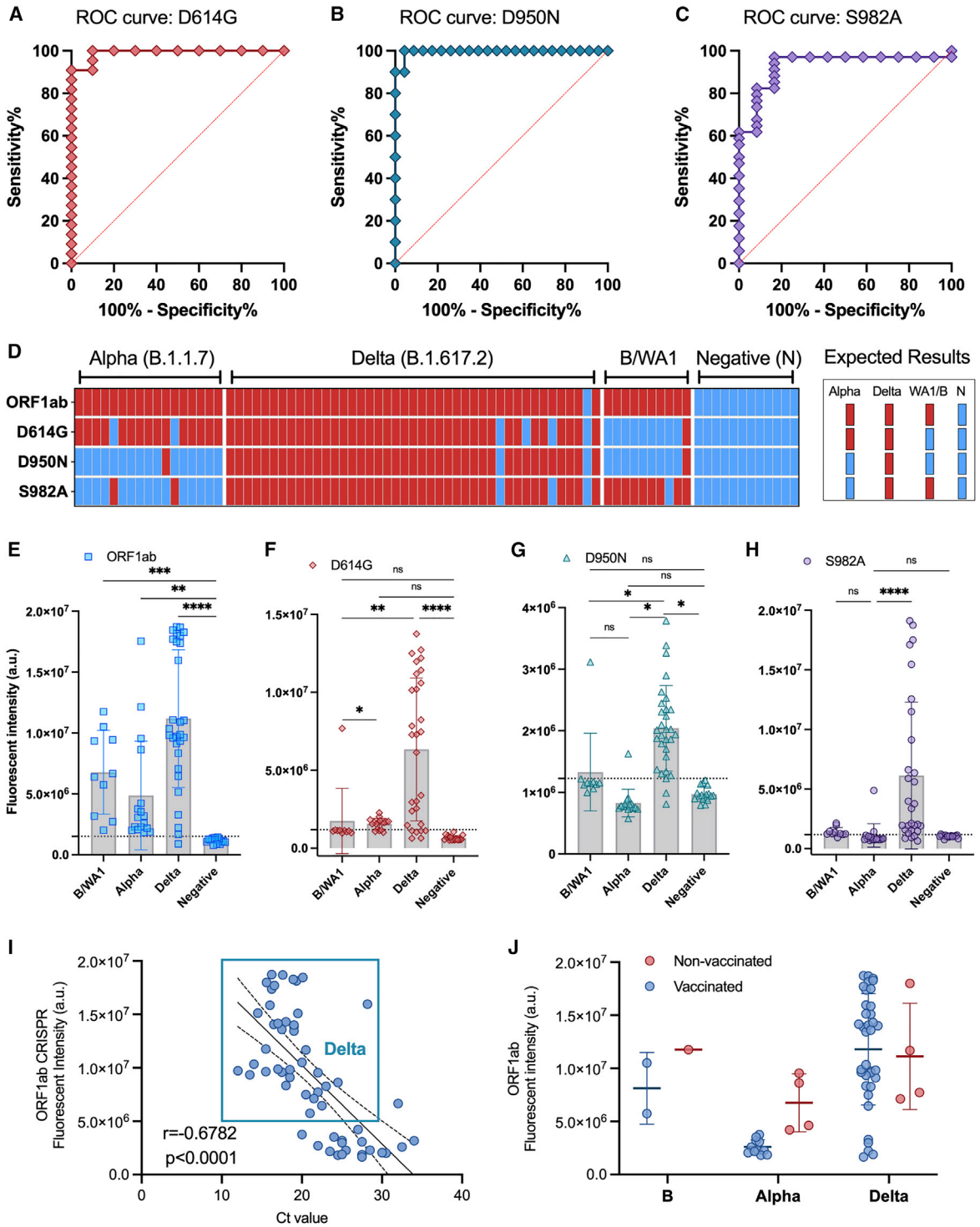

Figure 3. CRISPR detection of SARS-CoV-2 VOC strains in nasal swab samples

(A–C) ROC curves for CRISPR-FDS SNP assays targeting (A) D614G, (B) D950N, and (C) S982A.

(D) Heatmap summary of CRISPR-FDS assay-positive (red) and -negative (blue) results for the indicated targets in nasal swab samples with sequence data (16 Alpha, 44 Delta, 3 B strain), or that were collected months before the earliest reported VOC mutations (7 "B/WA1" samples), or which had negative qRT-PCR results (12 negative controls).

(E–H) Relative CRISPR-FDS signal intensity detected for ORF1ab or the indicated VOC SNPs in nasal swab samples of patients infected with SARS-CoV-2 B/WA1, Alpha, or Delta strains or with no evidence of SARS-CoV-2 infection. Positive CRISPR signal thresholds were defined as (E) the mean plus three times the SD of the negative control sample or (F–H) by the corresponding ROC analysis (A–C).

(legend continued on next page)

of the elevated signal detected in both assays, consistent with recent studies indicating higher viral load in nasal tissue of individuals infected with the SARS-CoV-2 Delta variant (Li et al., 2021). Most subjects involved in this study were vaccinated, and the limited number of unvaccinated individuals thus prevented accurate and robust evaluation of relative viral load in nasal swab samples via CRISPR-FDS ORF1ab signal intensity, although potential increased signals observed in unvaccinated patients infected with the B/WA1 strain or Alpha variant were not observed in patients infected with the Delta variant (Figure 3J).

Cellphone detection of COVID-19 SARS-CoV-2 mutations

Identification of SARS-CoV-2 variants currently requires that a subset of positive samples be selected and transported to a laboratory capable of routine large-scale NGS assays limiting the total sequencing capacity available for such analyses. This inefficient and expensive process has limited capacity and can delay the detection of rapid increases in new variants, limiting its ability to detect rapid increases in the incidence of new variants that can provide critical epidemiologic information. The assay approach described above can rapidly detect SARS-CoV-2 variants with high diagnostic sensitivity and specificity using resources available in most clinical diagnostic laboratories to expand variant screening capacity in areas served by these laboratories. However, the multi-step sample-handling procedure and equipment requirements of these assays may limit their translation in resource-limited settings.

We therefore streamlined the assay protocol by reducing the number of steps and adapting it to an RT-RPA assay format read by a smartphone device, an approach that we have previously reported can permit point-of-care SARS-CoV-2 diagnosis with a less than 1 h sample-to-answer time, including RNA purification (Figure 4A) (Ning et al., 2021). This analysis employed a smartphone device that we have previously reported can detect SARS-CoV-2 over a broad concentration range (1–10^5 copies/μL) with a limit of detection of <0.05 copies/μL using a similar assay approach (Ning et al., 2021) This device integrates a smartphone adaptor, external lens filter, 100 mW laser diode (465 nm), power switch, chip slot, and an emission filter. In this study this device was modified by replacing its original 525-nm band-pass filter with a 500-nm long range filter to enhance signal recovery and permit future use with additional dyes. Sample wells on assay chips read by this device were preloaded with target-specific gRNA and CRISPR reagents, loaded with the multiplex RT-RPA reaction product of a clinical sample, and then placed in the smartphone device for signal readout. Multiplex RT-RPA reactions that amplify the ORF1ab target region and S1 and S2 target amplicons containing SNPs for D614G and D905N and S982A are split and separately analyzed by CRISPR-FDS reactions on separate wells of an assay chip that is read by the smartphone device, where distinct patterns of positive signal for these four targets indicate the presence of specific SARS-CoV-2 strains or the absence of detectable virus.

A proof-of-principle study using this approach to analyze cultured virus isolates demonstrated a clear ability to distinguish the targeted SARS-CoV-2 Alpha and Delta VOC strains and the reference WA1 strain, but not other VOC strains that exhibit strain-specific SNPs (Figure 4B).

CRISPR-FDS signal detected by the cellphone device tended to exhibit similar relative intensity patterns among each strain for a given target region, with samples from individuals infected with Delta strain exhibiting higher signals for all markers than those infected with Alpha or B/WA1 (Figures 4C–4F).

An analysis of the 44 clinical samples in the original cohort with the remaining material (4 Alpha, 25 Delta, 9 B/WA1, and 6 SARS-CoV-2 negative cases) found that this approach exhibited high diagnostic sensitivity and specificity for identification of all SARS-CoV-2 strains (ORF1ab positive; 100%/100%), all VOC strains (D614G positive; 93.1%/93.3%), and Delta (D950N positive; 96%/94.7%) and Alpha (S982A-negative; 100%/92.5%) VOC strains (Figure 4G), although the reduced number of samples available decreased the statistical power of this analysis.

DISCUSSION

Improved methodologies are needed to evaluate strain-specific clinical outcomes of current and emerging VOCs to better inform treatment approaches, particularly in vulnerable populations, such as children, pregnant women, and immunosuppressed individuals (Chen et al., 2020a; Molloy and Bearer, 2020; Slimano et al., 2020). Most information regarding SARS-CoV-2 infection, including vaccine and treatment effectiveness, risk of long-term health effects, and re-infection risk, was determined before the widespread emergence of the VOCs, and must be reevaluated for each new VOC due to their potential phenotypic differences from the reference strains used to determine these parameters (Bian et al., 2021). Current sequencing approaches are not ideal for these efforts, however, since they are expensive, technically demanding, and lack the capacity for rapid high-throughput analyses required for these large-scale studies (Andreano and Rappuoli, 2021). We propose that CRISPR-FDS assays that target SNPs in PAM motifs and seed regions in most VOC strains identified to date can be used to meet this need, as indicated by the proof-of-concept studies described above.

SNPs are an extremely useful means of differentiating closely related nucleotide sequences but can be challenging to detect and differentiate with high sensitivity using rapid, cost-effective methods suitable for use in high-throughput applications. SNP detection methods can be divided into sequencing and PCR-based methods. Sequencing-based methods are not suitable for large screening studies, unlike PCR approaches, which tend to be less expensive and can exhibit higher capacity. PCR methods used for SNP analysis can be generally categorized into methods that rely on allele-specific primers to promote

(I) Linear correlation and 95% CI of Orf1ab CRISPR signal intensity with qRT-PCR Ct values for the SARS-CoV-2 N gene, where a box indicates a cluster of CRISPR and RT-qPCR signal from Delta variant samples.
(J) Relative CRISPR-FDS signal intensity for ORF1ab in patients infected with SARS-CoV-2 B, Alpha, or Delta with or without a history of full vaccination with the Pfizer SARS-CoV-2 mRNA vaccine. Cas12a incubation time was standardized at 15 min. *$p < 0.05$, **$p < 0.01$, ***$p < 0.005$, ****$p < 0.001$ by two-way ANOVA test.

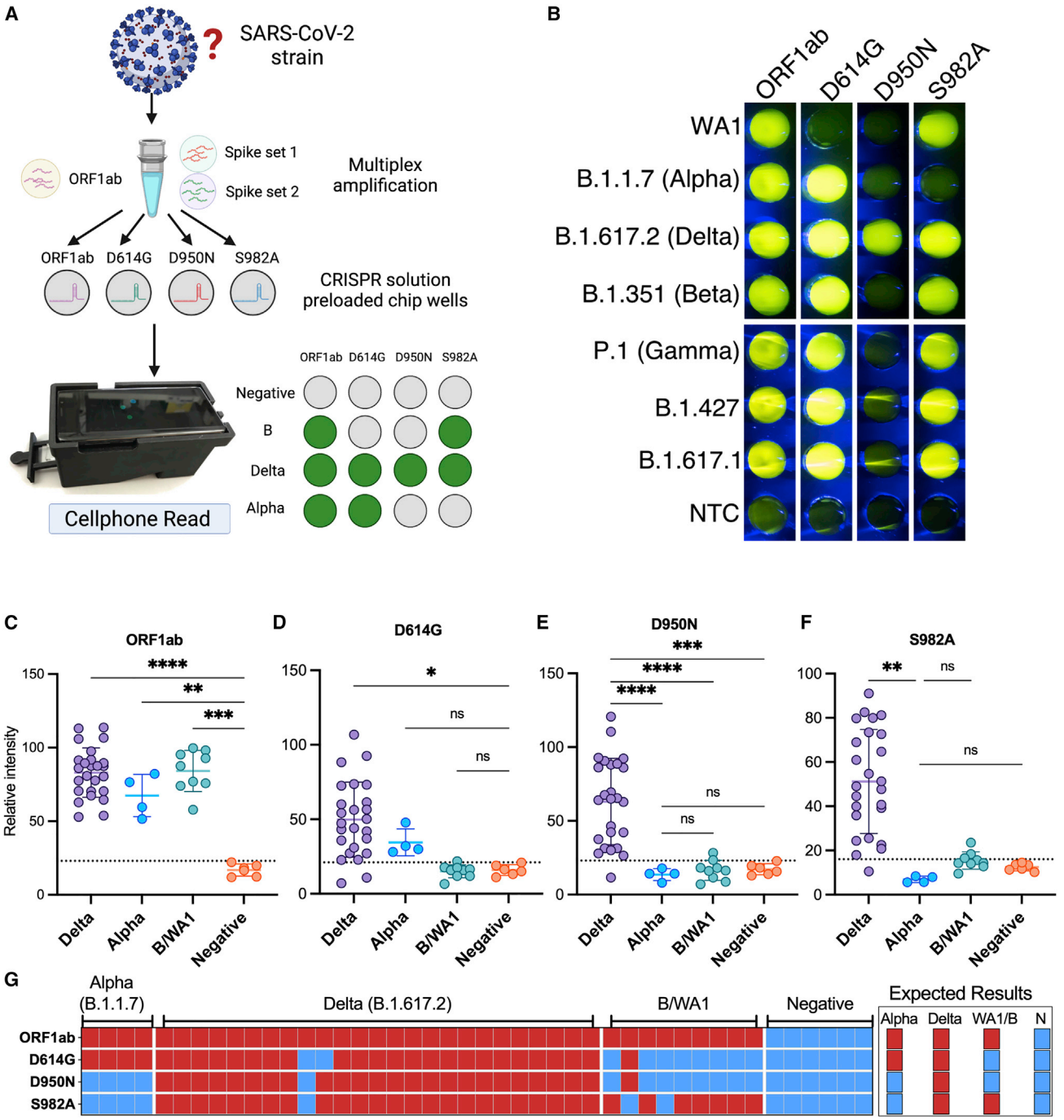

Figure 4. Smartphone detection of COVID-19 CRISPR mutation assay

(A) Schematic for smartphone-based detection of SARS-CoV-2, all VOC strains, and specific VOC strains. RNA from nasal swab samples is amplified by multiplex RT-RPA reactions, which are then split into microchip wells pre-loaded with guide RNA-CRISPR reagent mixtures, incubated at room temperature for 30 min, after which chips are loaded into the smartphone device and images of the CRISPR-FDS signal in each well is read by the smartphone and analyzed by ImageJ.

(B) Smartphone images of CRISPR-FDS assay microchip signal detected following a room temperature multiplex RT-RPA reaction to amplify the ORF1ab, S1, and S2 target regions.

(C–F) Relative signal intensity from nasal swab samples of patients infected with or without (negative) the indicated SARS-CoV-2 strains when analyzed by the RT-RPA CRISPR-FDS smartphone assays for the ORF1ab, spike D614G, D950N, and S982A targets.

(G) Heatmap summary of CRISPR-FDS assay-positive (red) and -negative (blue) results for the indicated targets in nasal swab samples of patients with Alpha, Delta, or B/WA1 SARS-CoV-2 infections.

selective amplification of the target SNP sequence or that employ melting curve analyses to differentiate between amplicons that contain different SNPs. The first approach employs allele-specific primers that either exhibit strong selectivity for a mutant allele to promote its amplification or for a wild-type allele to block its amplification and promote selective amplification of the mutant allele, with the blocking primers used in the second approach containing a 3′ dideoxy modification to prevent primer elongation (Matsuda, 2017). The second approach relies upon a differential denaturation rate of the double-strand DNA containing the SNP of interest upon exposure to a temperature gradient, as detected by a corresponding loss of intercalation by SYBR Green dye or binding of a quenched fluorescent probe. SNP detection in this approach depends on the length and sequence, particularly the GC base content and distribution, of the target amplicon or probe target. Differentiation of specific target SNPs by either differential amplification or melting curve analysis may require sequence-specific adjustment of the assay parameters and be limited by the specific nucleotide altered by the SNP.

In this study, we demonstrate that we can employ a CRISPR-FDS assay approach to efficiently detect SARS-CoV-2 SNPs that alter variant-specific PAM motifs and their seed regions, which can markedly affect the cleavage activity of the Cas12a enzyme complex (Chen et al., 2018), while previous studies have indicated that CRISPR can detect SNPs that do not affect these regions, albeit with lower efficiency, or deletions (Casati et al., 2021; de Puig et al., 2021). This targeting flexibility makes CRISPR-FDS assays that target strain-specific SARS-CoV-2 mutations ideal candidates for future VOC screening efforts.

Multiple SNPs, and three deletions, affecting PAM motifs and their seed regions were detected in the spike gene sequence of all VOCs analyzed in this study, to uniquely distinguish them, and thus it appears likely similar SNPs in the spike gene of future VOCs or VOIs should have the similar differential ability. The spike gene was selected for this analysis since it is the predominant surface protein of SARS-CoV-2 and serves as its receptor for cell entry, and thus should be under significant selective pressure. However, if necessary, SNPs or deletions that target PAM or seed regions in other SARS-CoV-2 gene regions, could be analyzed to permit discrimination of strains that do not contain unique mutations with spike gene sequence. Furthermore, it should also be possible to use a PCR primer to insert a PAM motif next to a variant-specific SNP to create a *de novo* seed region mutation (Chen et al., 2021b).

We believe that this approach should allow rapid assay development of the detection of new and emerging variants through a standard screening process in which their sequence is aligned against other know strains to identify mutations affecting Cas12a PAM motifs (TTTV) or seed regions within the first six bases downstream of an intact PAM sequence. For assays targeting SNPs in a Cas12a seed region, an additional sequence mismatch should be added to the gRNA sequence within one to two nucleotides of the SNP site to ensure the destabilization of gRNA/Cas12a binding and a robust difference in its cleavage-induced assay signal. Notably, multiple SNPs can often be captured within a single amplicon, as we indicate in our sequence analysis of current VOC strains, and demonstrate with our D950N and S982 assays. Given knowledge of the requirements for optimal PAM and sequences it should be possible to identify assay targets in virus sequence with good confidence, or to identify a potential strain-specific SNP with a seed sequence newly defined by the insertion of an adjacent PAM site by an amplicon primer (Chen et al., 2018). Following target identification, the validation of new variant assays is primarily limited by the time required to obtain the new gRNA sequences (~5 days when purchased from commercial vendors), the availability or synthesis of a reference sample, and the availability of patient samples for clinical validation. Analytical assay validation steps (e.g., titration of primer, gRNA, and Cas12a concentration and assay temperate) are routine and can be rapidly performed in batch analyses. Initial validation studies for new assays could thus require less than a week if all these materials are available.

Previous CRISPR-based detection assays designed to detect SARS-CoV-2 variant strains did not test multiple targets using clinical samples due to lack of sample availability, and targeted deletions or seed region mutations (Meng et al., 2021; Wang et al., 2021b; Zhang et al., 2020). In this study we evaluate the ability of a multiplex CRISPR-FDS assay to detect and distinguish the SARS-CoV-2 Alpha and Delta strains, which were dominant in our patient population at the time of sample collection and indicate that SNPs that create or disrupt PAM motifs are another source of effective markers to distinguish SARS-CoV-2 variant strains.

The ability to identify specific variant strains at diagnosis has been proposed to have significant implications for clinical treatment decisions (Fang and Schooley, 2020; Visvikis-Siest et al., 2020). Evidence-based practice relies on large-scale research studies that provide clear guidelines for ideal treatment in patients with particular disease-risk factors or comorbidities (Xu et al., 2020) and clear and reliable evidence-based guidelines for the treatment of SARS-CoV-2 VOC strains cannot be generated without widespread identification of patients with specific VOCs and correlation of these VOCs with specific phenotypes, treatment responses, and outcomes in conjunction with other clinical information.

In this study, VOC-specific SNPs that altered PAM and seed regions were employed to identify clinical samples from individuals determined to have SARS-CoV-2 Alpha or Delta strain infection based on sequence information. Another useful strategy, however, is to target mutations shared by multiple VOC or VOI strains to identify all individuals infected with strains that carry this mutation as broader means to screen for variants belonging to these lineages, which may inform sampling approaches for sequencing efforts required to identify new variants. We targeted the D614G for this purpose but multiple other SNPs that appear to increase virus transmissibility or the evasion of antibody responses (e.g., N501Y, E484K, L452R, and K417N-T) could be important markers to inform clinical decisions, since they may differentially affect response to specific treatments (Jensen et al., 2021).

One limitation of this study is that it employed small sample cohorts to estimate the diagnostic sensitivity and specificity of the general, VOC pan-specific, and strain-specific VOC assays due to limited sample availability, which may have limited the accuracy of these measurements.

A second limitation is that this assay approach still requires population-based sequencing efforts to identify new VOI or

VOC strains and their unique SNPs to allow the development of strain-specific CRISPR-FDS assays. Once such strain has been detected; however, strain-specific CRISPR-FDS assays can be rapidly used to detect the early emergence of new clusters of variant cases that might not be detected until much later by current efforts that use population-sampling approaches to generate specimen cohorts for sequence analysis. Furthermore, while such CRISPR assays cannot directly identify the emergence of new strains, they may be able to detect and track the rise of newly emerging dominant strains by detecting a decrease in the percentage of positive results for a dominant variant strain among patients with SARS-CoV-2 infections (Challen et al., 2021b).

We believe our SNP detection strategy can be integrated into future CRISPR-based POC tests for use in resource-limited settings, but this will require overcoming several obstacles. These include optimizing extraction-free isothermal reaction conditions and fluid handling on an inexpensive device capable of sensitive assay readout to reduce sample processing and liquid handling requirements that increase the chance for aerosol contamination. Several studies have shown that it is possible to address each of these issues. For example, RNA extraction-based and extraction-free SARS-CoV-2 assays that employ RT-PCR (Park et al., 2021; Smyrlaki et al., 2020) or CRISPR (Park et al., 2021; Garcia-Venzor et al., 2021; Ning et al., 2021) can have comparable sensitivity and specificity. Small and inexpensive microfluidic or electronic devices can also be used to automate or control reagent mixing and reaction temperature (de Puig et al., 2021; Chen et al., 2021a, 2021b) and one-pot assays that combine DNA amplification and CRISPR reactions in single tubes (Chen et al., 2020c; Joung et al., 2020) can minimize sample handling and aerosol production to reduce contamination via amplicon transfer. We therefore believe it should be possible to adapt our current assay to a POC test that can sensitively detect infections caused by specific SARS-CoV-2 VOC strains.

Finally, this study analyzed the analytical and diagnostic performance of only three CRISPR-FDS assays that targeted pan-specific and variant-specific SNPs, which revealed similar results, but it is possible that CRISPR-FDS assays targeting different SNPs in alternate PAM motif sites or their seed regions could exhibit variable performance. This limitation was partly due to the number of samples available for analysis, and further studies using more and larger variant cohorts are necessary to address this issue.

New SARS-CoV-2 variants are likely to arise as the pandemic continues, and new approaches are needed to more rapidly detect strains that exhibit a competitive advantage as they begin to displace existing dominant strains. We propose that the adaptability of the multiplex detection approach outlined in this study has the potential to address the need to rapidly characterize the phenotype and clinical response of such variants.

Limitations of the study

This VOC detection approach requires that analyzed mutations alter a PAM or its associated seed sequence to create or disrupt a CRISPR-Cas12a cleavage sites, and a particular SNP of interest may not meet these conditions. This therefore requires that the genome of a VOC strain must first be sequenced to identify mutations that meet these criteria. Finally, this assay now requires liquid handling steps that may limit its utility in point-of-care settings, but it could be modified for this application by adapting it to an RNA extraction-free assay performed on microfluidic chips that permit automatic reagent mixing.

STAR★METHODS

Detailed methods are provided in the online version of this paper and include the following:

- KEY RESOURCES TABLE
- RESOURCE AVAILABILITY
  - Lead contact
  - Materials availability
  - Data and code availability
- EXPERIMENTAL MODEL AND SUBJECT DETAILS
  - Cultured virus samples
  - Nasal swab collection
- METHOD DETAILS
  - RNA extraction
  - Isolation free detection of SARS-CoV-2 in solution
  - Nucleic acid amplification
  - CRISPR detection assay
  - Standard curve and limit of detection (LoD)
  - Cellphone detection for quantitative point-of-care readout
- QUANTIFICATION AND STATISTICAL ANALYSIS

SUPPLEMENTAL INFORMATION

Supplemental information can be found online at https://doi.org/10.1016/j.crmeth.2022.100173.

ACKNOWLEDGMENTS

We would like to thank Sanchita Das (NIH) for providing clinical samples. T.Y.H. wants to give thanks for the generous support of the Weatherhead Presidential Endowment fund, N.J.M. wants to thank the National Institutes of Health for grant P51OD01110459. Some figures were created using Biorender.com.

AUTHOR CONTRIBUTIONS

Conceptualization, B.N. and T.Y.H.; methodology, B.N. and B.M.Y.; investigation, T.Y.H.; visualization, B.N. and B.M.Y.; funding acquisition, T.Y.H. and N.J.M.; project administration, T.Y.H.; supervision, T.Y.H.; writing – original draft, B.M.Y. and B.N.; writing – review & editing, C.J.L. and T.Y.H.

DECLARATION OF INTERESTS

T.Y.H. and C.J.L. are the shareholders of Nanopin Technologies Inc. T.Y.H. is a co-founder of Nanopin Technologies Inc. and a member of its scientific advisory board. B.N. and T.Y.H. are the inventors of a patent entitled "CRISPR-based assay for detecting SARS-CoV-2 in samples prior related applications."

Received: September 13, 2021
Revised: October 26, 2021
Accepted: January 31, 2022
Published: February 7, 2022

REFERENCES

Andreano, E., and Rappuoli, R. (2021). SARS-CoV-2 escaped natural immunity, raising questions about vaccines and therapies. Nat. Med. *27*, 759–761.

Arizti-Sanz, J., Freije, C.A., Stanton, A.C., Petros, B.A., Boehm, C.K., Siddiqui, S., Shaw, B.M., Adams, G., Kosoko-Thoroddsen, T.-S.F., Kemball, M.E., et al. (2020). Streamlined inactivation, amplification, and Cas13-based detection of SARS-CoV-2. Nat. Commun. *11*, 5921. https://doi.org/10.1038/s41467-020-19097-x.

Baum, A., Fulton, B.O., Wloga, E., Copin, R., Pascal, K.E., Russo, V., Giordano, S., Lanza, K., Negron, N., and Ni, M. (2020). Antibody cocktail to SARS-CoV-2 spike protein prevents rapid mutational escape seen with individual antibodies. Science *369*, 1014–1018.

Bian, L., Gao, F., Zhang, J., He, Q., Mao, Q., Xu, M., and Liang, Z. (2021). Effects of SARS-CoV-2 variants on vaccine efficacy and response strategies. Expert Rev. Vaccin. *20*, 365–373.

Broughton, J.P., Deng, X., Yu, G., Fasching, C.L., Servellita, V., Singh, J., Miao, X., Streithorst, J.A., Granados, A., and Sotomayor-Gonzalez, A. (2020). CRISPR–Cas12-based detection of SARS-CoV-2. Nat. Biotechnol. *38*, 870–874.

Brown, K.A., Gubbay, J., Hopkins, J., Patel, S., Buchan, S.A., Daneman, N., and Goneau, L.W. (2021). S-gene target failure as a marker of variant B. 1.1. 7 among SARS-CoV-2 isolates in the greater Toronto area, December 2020 to March 2021. JAMA *325*, 2115–2116.

Casati, B., Verdi, J.P., Hempelmann, A., Kittel, M., Klaebisch, A.G., Welker, S., Asthana, S., Boskovic, P., Man, K.H., and Radlwimmer, B. (2021). ADESSO detects SARS-CoV-2 and its variants: extensive clinical validation of an optimised CRISPR-Cas13-based COVID-19 test. Preprint at medRxiv.

Challen, R., Brooks-Pollock, E., Read, J.M., Dyson, L., Tsaneva-Atanasova, K., and Danon, L. (2021a). Increased hazard of mortality in cases compatible with SARS-CoV-2 variant of concern 202012/1-a matched cohort study. Preprint at medRxiv.

Challen, R., Dyson, L., Overton, C.E., Guzman-Rincon, L.M., Hill, E.M., Stage, H.B., Brooks-Pollock, E., Pellis, L., Scarabel, F., and Pascall, D.J. (2021b). Early epidemiological signatures of novel SARS-CoV-2 variants: establishment of B. 1.617. 2 in England. Preprint at medRxiv.

Chen, F.-E., Lee, P.-W., Trick, A.Y., Park, J.S., Chen, L., Shah, K., Mostafa, H., Carroll, K.C., Hsieh, K., and Wang, T.-H. (2021a). Point-of-care CRISPR-Cas-assisted SARS-CoV-2 detection in an automated and portable droplet magnetofluidic device. Biosens. Bioelectron. *190*, 113390. https://doi.org/10.1016/j.bios.2021.113390.

Chen, J.S., Ma, E., Harrington, L.B., Da Costa, M., Tian, X., Palefsky, J.M., and Doudna, J.A. (2018). CRISPR-Cas12a target binding unleashes indiscriminate single-stranded DNase activity. Science *360*, 436–439.

Chen, L., Li, Q., Zheng, D., Jiang, H., Wei, Y., Zou, L., Feng, L., Xiong, G., Sun, G., and Wang, H. (2020a). Clinical characteristics of pregnant women with Covid-19 in Wuhan, China. New Engl. J. Med. *382*, e100.

Chen, P., Zhou, J., Wan, Y., Liu, H., Li, Y., Liu, Z., Wang, H., Lei, J., Zhao, K., and Zhang, Y. (2020b). A Cas12a ortholog with stringent PAM recognition followed by low off-target editing rates for genome editing. Genome Biol. *21*, 1–13.

Chen, Y., Mei, Y., and Jiang, X. (2021b). Universal and high-fidelity DNA single nucleotide polymorphism detection based on a CRISPR/Cas12a biochip. Chem. Sci. *12*, 4455–4462.

Chen, Y., Shi, Y., Chen, Y., Yang, Z., Wu, H., Zhou, Z., Li, J., Ping, J., He, L., Shen, H., et al. (2020c). Contamination-free visual detection of SARS-CoV-2 with CRISPR/Cas12a: a promising method in the point-of-care detection. Biosens. Bioelectron. *169*, 112642. https://doi.org/10.1016/j.bios.2020.112642.

Chiara, M., D'Erchia, A.M., Gissi, C., Manzari, C., Parisi, A., Resta, N., Zambelli, F., Picardi, E., Pavesi, G., and Horner, D.S. (2021). Next generation sequencing of SARS-CoV-2 genomes: challenges, applications and opportunities. Brief. Bioinform. *22*, 616–630.

Davies, N.G., Abbott, S., Barnard, R.C., Jarvis, C.I., Kucharski, A.J., Munday, J.D., Pearson, C.A., Russell, T.W., Tully, D.C., and Washburne, A.D. (2021a). Estimated transmissibility and impact of SARS-CoV-2 lineage B. 1.1. 7 in England. Science *372*, 149.

Davies, N.G., Jarvis, C.I., Edmunds, W.J., Jewell, N.P., Diaz-Ordaz, K., and Keogh, R.H. (2021b). Increased mortality in community-tested cases of SARS-CoV-2 lineage B. 1.1. 7. Nature *593*, 270–274.

de Puig, H., Lee, R.A., Najjar, D., Tan, X., Soekensen, L.R., Angenent-Mari, N.M., Donghia, N.M., Weckman, N.E., Ory, A., and Ng, C.F. (2021). Minimally instrumented SHERLOCK (miSHERLOCK) for CRISPR-based point-of-care diagnosis of SARS-CoV-2 and emerging variants. Sci. Adv. *7*, eabh2944.

Fang, F.C., and Schooley, R.T. (2020). Treatment of COVID-19-evidence-based or personalized medicine? Clin. Infect. Dis.

Garcia-Venzor, A., Rueda-Zarazua, B., Marquez-Garcia, E., Maldonado, V., Moncada-Morales, A., Olivera, H., Lopez, I., Zuñiga, J., and Melendez-Zajgla, J. (2021). SARS-CoV-2 direct detection without RNA isolation with loop-mediated isothermal amplification (LAMP) and CRISPR-Cas12. Front. Med. *8*, 125.

Gravagnuolo, A.M., Faqih, L., Cronshaw, C., Wynn, J., Klapper, P., and Wigglesworth, M. (2021). High throughput diagnostics and dynamic risk assessment of SARS-CoV-2 variants of concern. EBioMedicine *70*, 103540.

Hafeez, S., Din, M., Zia, F., Ali, M., and Shinwari, Z.K. (2021). Emerging concerns regarding COVID-19; second wave and new variant. J. Med. Virol. *93*, 4108.

Horby, P., Huntley, C., Davies, N., Edmunds, J., Ferguson, N., Medley, G., and Semple, C. (2021). NERVTAG paper on COVID-19 variant of concern B.1.1.7 (Department of Health and Social Care), pp. 1–9.

Hou, Y.J., Chiba, S., Halfmann, P., Ehre, C., Kuroda, M., Dinnon, K.H., Leist, S.R., Schäfer, A., Nakajima, N., and Takahashi, K. (2020). SARS-CoV-2 D614G variant exhibits efficient replication ex vivo and transmission in vivo. Science *370*, 1464–1468.

Huang, X., Zhang, F., Zhu, K., Lin, W., and Ma, W. (2021a). dsmCRISPR: dual synthetic mismatches CRISPR/Cas12a-based detection of SARS-CoV-2 D614G mutation. Virus Res., 198530.

Huang, Z., Ning, B., Yang, H.S., Youngquist, B.M., Niu, A., Lyon, C.J., Beddingfield, B.J., Fears, A.C., Monk, C.H., and Murrell, A.E. (2021b). Sensitive tracking of circulating viral RNA through all stages of SARS-CoV-2 infection. J. Clin. Invest. *131*, e146031.

Huang, Z., Tian, D., Liu, Y., Lin, Z., Lyon, C., Lai, W., Fusco, D., Drouin, A., Yin, X., and Hu, T. (2020). Ultra-sensitive and high-throughput CRISPR-Powered COVID-19 diagnosis. Biosens. Bioelectron. *164*, 112316.

Jangra, S., Ye, C., Rathnasinghe, R., Stadlbauer, D., Alshammary, H., Amoako, A.A., Awawda, M.H., Beach, K.F., Bermúdez-González, M.C., Chernet, R.L., et al. (2021). SARS-CoV-2 spike E484K mutation reduces antibody neutralisation. Lancet Microbe *2*, e283–e284. https://doi.org/10.1016/S2666-5247(21)00068-9.

Jayamohan, H., Lambert, C.J., Sant, H.J., Jafek, A., Patel, D., Feng, H., Beeman, M., Mahmood, T., Nze, U., and Gale, B.K. (2021). SARS-CoV-2 pandemic: a review of molecular diagnostic tools including sample collection and commercial response with associated advantages and limitations. Anal. Bioanal. Chem. *413*, 49–71.

Jensen, B., Luebke, N., Feldt, T., Keitel, V., Brandenburger, T., Kindgen-Milles, D., Lutterbeck, M., Freise, N.F., Schoeler, D., and Haas, R. (2021). Emergence of the E484K mutation in SARS-COV-2-infected immunocompromised patients treated with bamlanivimab in Germany. Lancet Reg. Health Eur. *8*, 100164.

Joung, J., Ladha, A., Saito, M., Kim, N.-G., Woolley, A.E., Segel, M., Barretto, R.P.J., Ranu, A., Macrae, R.K., Faure, G., et al. (2020). Detection of SARS-CoV-2 with SHERLOCK one-pot testing. New Engl. J. Med. *383*, 1492–1494. https://doi.org/10.1056/NEJMc2026172.

Korber, B., Fischer, W.M., Gnanakaran, S., Yoon, H., Theiler, J., Abfalterer, W., Hengartner, N., Giorgi, E.E., Bhattacharya, T., and Foley, B. (2020). Tracking changes in SARS-CoV-2 spike: evidence that D614G increases infectivity of the COVID-19 virus. Cell *182*, 812–827.e9.

Li, B., Deng, A., Li, K., Hu, Y., Li, Z., Xiong, Q., Liu, Z., Guo, Q., Zou, L., and Zhang, H. (2021). Viral infection and transmission in a large well-traced outbreak caused by the Delta SARS-CoV-2 variant. Preprint at MedRxiv.

Li, Q., Wu, J., Nie, J., Zhang, L., Hao, H., Liu, S., Zhao, C., Zhang, Q., Liu, H., and Nie, L. (2020). The impact of mutations in SARS-CoV-2 spike on viral infectivity and antigenicity. Cell *182*, 1284–1294.e9.

Liu, Z., VanBlargan, L.A., Bloyet, L.-M., Rothlauf, P.W., Chen, R.E., Stumpf, S., Zhao, H., Errico, J.M., Theel, E.S., and Liebeskind, M.J. (2021). Identification of SARS-CoV-2 spike mutations that attenuate monoclonal and serum antibody neutralization. Cell Host Microbe *29*, 477–488.e4.

Lopez Bernal, J., Andrews, N., Gower, C., Gallagher, E., Simmons, R., Thelwall, S., Stowe, J., Tessier, E., Groves, N., and Dabrera, G. (2021). Effectiveness of Covid-19 vaccines against the B. 1.617. 2 (Delta) variant. New Engl. J. Med. *385*, 585–594.

Matsuda, K. (2017). PCR-based detection methods for single-nucleotide polymorphism or mutation: real-time PCR and its substantial contribution toward technological refinement. Adv. Clin. Chem. *80*, 45–72.

Meng, Q., Wang, X., Wang, Y., Dang, L., Liu, X., Ma, X., Chi, T., Wang, X., Zhao, Q., and Yang, G. (2021). Detection of the SARS-CoV-2 D614G mutation using engineered Cas12a guide RNA. Biotechnol. J. *16*, 2100040.

Molloy, E.J., and Bearer, C.F. (2020). COVID-19 in children and altered inflammatory responses. Pediatr. Res. *88*, 340–341.

Myhrvold, C., Freije, C.A., Gootenberg, J.S., Abudayyeh, O.O., Metsky, H.C., Durbin, A.F., Kellner, M.J., Tan, A.L., Paul, L.M., and Parham, L.A. (2018). Field-deployable viral diagnostics using CRISPR-Cas13. Science *360*, 444–448.

Nagy, Á., Pongor, S., and Győrffy, B. (2021). Different mutations in SARS-CoV-2 associate with severe and mild outcome. Int. J. Antimicrob. Agents *57*, 106272.

Ning, B., Yu, T., Zhang, S., Huang, Z., Tian, D., Lin, Z., Niu, A., Golden, N., Hensley, K., and Threeton, B. (2021). A smartphone-read ultrasensitive and quantitative saliva test for COVID-19. Sci. Adv. *7*, eabe3703.

Palaz, F., Kalkan, A.K., Tozluyurt, A., and Ozsoz, M. (2021). CRISPR-based tools: alternative methods for the diagnosis of COVID-19. Clin. Biochem. *89*, 1.

Pardee, K., Green, A.A., Takahashi, M.K., Braff, D., Lambert, G., Lee, J.W., Ferrante, T., Ma, D., Donghia, N., Fan, M., et al. (2016). Rapid, low-cost detection of Zika virus using programmable biomolecular components. Cell *165*, 1255–1266. https://doi.org/10.1016/j.cell.2016.04.059.

Park, J.S., Hsieh, K., Chen, L., Kaushik, A., Trick, A.Y., and Wang, T.-H. (2021). Digital CRISPR/Cas-Assisted assay for rapid and sensitive detection of SARS-CoV-2. Adv. Sci. *8*, 2003564. https://doi.org/10.1002/advs.202003564.

Plante, J.A., Liu, Y., Liu, J., Xia, H., Johnson, B.A., Lokugamage, K.G., Zhang, X., Muruato, A.E., Zou, J., and Fontes-Garfias, C.R. (2021). Spike mutation D614G alters SARS-CoV-2 fitness. Nature *592*, 116–121.

Ramachandran, A., Huyke, D.A., Sharma, E., Sahoo, M.K., Huang, C., Banaei, N., Pinsky, B.A., and Santiago, J.G. (2020). Electric field-driven microfluidics for rapid CRISPR-based diagnostics and its application to detection of SARS-CoV-2. Proc. Natl. Acad. Sci. *117*, 29518. https://doi.org/10.1073/pnas.2010254117.

Slimano, F., Baudouin, A., Zerbit, J., Toulemonde-Deldicque, A., Thomas-Schoemann, A., Chevrier, R., Daouphars, M., Madelaine, I., Pourroy, B., and Tournamille, J.-F. (2020). Cancer, immune suppression and Coronavirus disease-19 (COVID-19): need to manage drug safety (French Society for Oncology pharmacy [SFPO] guidelines). Cancer Treat. Rev. *88*, 102063.

Smyrlaki, I., Ekman, M., Lentini, A., Rufino de Sousa, N., Papanicolaou, N., Vondracek, M., Aarum, J., Safari, H., Muradrasoli, S., Rothfuchs, A.G., et al. (2020). Massive and rapid COVID-19 testing is feasible by extraction-free SARS-CoV-2 RT-PCR. Nat. Commun. *11*, 4812. https://doi.org/10.1038/s41467-020-18611-5.

Teng, F., Guo, L., Cui, T., Wang, X.-G., Xu, K., Gao, Q., Zhou, Q., and Li, W. (2019). CDetection: CRISPR-Cas12b-based DNA detection with sub-attomolar sensitivity and single-base specificity. Genome Biol. *20*, 132. https://doi.org/10.1186/s13059-019-1742-z.

Visvikis-Siest, S., Theodoridou, D., Kontoe, M.-S., Kumar, S., and Marschler, M. (2020). Milestones in personalized medicine: from the ancient time to nowadays—the provocation of COVID-19. Front. Genet. *11*, 1442.

Volz, E., Mishra, S., Chand, M., Barrett, J.C., Johnson, R., Geidelberg, L., Hinsley, W.R., Laydon, D.J., Dabrera, G., and O'Toole, Á. (2021). Transmission of SARS-CoV-2 Lineage B. 1.1. 7 in England: insights from linking epidemiological and genetic data. Preprint at MedRxiv, 2020.2012. 2030.20249034.

Wang, P., Nair, M.S., Liu, L., Iketani, S., Luo, Y., Guo, Y., Wang, M., Yu, J., Zhang, B., and Kwong, P.D. (2021a). Antibody resistance of SARS-CoV-2 variants B. 1.351 and B. 1.1. 7. Nature *593*, 130–135.

Wang, Y., Zhang, Y., Chen, J., Wang, M., Zhang, T., Luo, W., Li, Y., Wu, Y., Zeng, B., and Zhang, K. (2021b). Detection of SARS-CoV-2 and its mutated variants via CRISPR-Cas13-based transcription amplification. Anal. Chem. *93*, 3393–3402.

Wibmer, C.K., Ayres, F., Hermanus, T., Madzivhandila, M., Kgagudi, P., Oosthuysen, B., Lambson, B.E., De Oliveira, T., Vermeulen, M., and Van der Berg, K. (2021). SARS-CoV-2 501Y. V2 escapes neutralization by South African COVID-19 donor plasma. Nat. Med. *27*, 622–625.

Xu, G., Yang, Y., Du, Y., Peng, F., Hu, P., Wang, R., Yin, M., Li, T., Tu, L., and Sun, J. (2020). Clinical pathway for early diagnosis of COVID-19: updates from experience to evidence-based practice. Clin. Rev. Allergy Immunol. *59*, 89–100.

Zhang, Y., Xi, H., and Juhas, M. (2020). Biosensing detection of the SARS-CoV-2 D614G mutation. Trends Genet. *37*, 299–302.

STAR★METHODS

KEY RESOURCES TABLE

REAGENT or RESOURCE	SOURCE	IDENTIFIER
Bacterial and virus strains		
A	BEI Resources	Cat#NR-52281
B.1.1.7	BEI Resources	Cat#NR-55461
B.1.35.1	BEI Resources	Cat#NR-55282
P.1	BEI Resources	Cat#NR-54982
B.1.427	BEI Resources	Cat#NR-55308
B.1.617.1	BEI Resources	Cat#NR-55486
B.1.617.2	BEI Resources	Cat#NR-55611
Biological samples		
Nasal swab samples	Tulane Molecular Pathology	IRB#2020-595
Chemicals, peptides, and recombinant proteins		
QuickExtract DNA Extraction Solution	Lucigen	Cat#QE09050
Platinum SuperFi PCR Master Mix	Invitrogen	Cat#12358010
SuperScript IV Reverse Transcriptase	Invitrogen	Cat#18090010
NEBuffer 2.1	NEB	Cat#B7202
EnGen Lba Cas12a (Cpf1)	NEB	Cat#M0653
Critical commercial assays		
Quick-DNA/ RNA Viral Kit	Zymo Research	Cat#C7020
MagMAX DNA Multi-Sample Ultra 2.0	Applied Biosystems	Cat#A36570
RPA reagents	TwistDx	Cat#TABAS03KIT
Oligonucleotides		
See Table S1 for oligonucleotide sequences	Integrated DNA Technologies (IDT)	N/A
Software and algorithms		
GraphPad Prism 8	GraphPad	https://www.graphpad.com/scientific-software/prism/
Other		
Nasal swabs	Zymo Research	Cat#R1119-B
96 Half Area Well Solid Black Flat Bottom Microplate	Corning	Cat#3875
Samsung Galaxy S9	Samsung	https://www.samsung.com/global/galaxy/galaxy-s9/
525nm CWL, 25mm Dia, 15nm Bandwidth, OD 6 Fluorescence Filter	Edmund Optics	Cat#86-354
SpectraMax i3x Multi-Mode Microplate Reader	Molecular Devices	https://www.moleculardevices.com/products/microplate-readers/multi-mode-readers/spectramax-i3x-readers#gref
12.5mm Dia. x 50.0mm FL, VIS 0° Coated, Plano-Convex Lens	Edmund Optics	Cat#38-296
465nm, 100mW blue laser diode	DTR's Laser Shop	Cat#NUBM07-465nm

RESOURCE AVAILABILITY

Lead contact

Further information and requests for resources and reagents should be directed to and will be fulfilled by the lead contact, Tony Hu (tonyhu@tulane.edu).

Materials availability

This study did not generate new unique reagents.

Data and code availability

- All data reported in this paper will be shared by the lead contact upon request
- This paper does not report original code.
- Information required to reanalyze the data reported in this paper is available from the lead contact upon request.

EXPERIMENTAL MODEL AND SUBJECT DETAILS

Cultured virus samples

Variant viral samples were purchased from BEI Resources with their associated catalog number in Table S2 and in the key resources table.

Nasal swab collection

A total of 82 nasal swab (Zymo Research Cat#R1119-B) specimens were collected based on clinical indications and current CDC guidance from Tulane Molecular Pathology in New Orleans, LA from July 7th to August 8th, 2020, in accordance with an approved institutional review board (IRB#2020-595) protocol with written informed consent. Nasal swab samples from 12 uninfected individuals and 71 individuals with SARS-CoV-2 infections (17 Alpha, 44 Delta, and 10 WA1/B strains). The gender, age, and vaccination status information for individuals tested is in Table S4. For 8 individuals tested, the vaccination status is unknown because there was no vaccination record or the individual refused to disclose vaccination status. All nasal swab samples were tested with the CDC 2019-nCoV Real-Time RT-PCR Diagnostic Panel (EUA) by the Tulane Molecular Pathology Lab.

METHOD DETAILS

RNA extraction

For cultured virus samples, 50 uL RNA was extracted from 100 uL viral seed stock (BEI resources) using the Zymo Quick-DNA/RNA Viral Kit (D7020). For clinical samples, 100 μL of RNA were extracted from 200 μL nasal swabs using the MagMAX DNA Multi-Sample Ultra 2.0 Kit (Applied Biosystems^{TM} A36570). Extracted RNA was stored at −80°C until analysis.

Isolation free detection of SARS-CoV-2 in solution

The ability of CRISPR-FDS assays to directly detect SARS-CoV-2 RNA in unprocessed samples was examined by adding of lysis buffer to virus culture samples that were then directly analyzed without RNA extraction. In this approach, 25 μL QuickExtract^{TM} DNA Extraction Solution (Lucigen) was mixed with 5 μL of virus culture sample supernatant that was centrifuged to remove cellular debris, and then incubated at 37°C for 10 min to release viral RNA. 5 μL of the lysed sample was mixed with a RT-RPA solution described below and incubated at 37°C and detected by addition of a 10 μL mixture containing a CRISPR-FDS reaction mixture.

Nucleic acid amplification

An amplification step of either RT-PCR or RT-RPA is used before CRISPR detection. For RT-PCR, mix composed of 12.5 μL 2X Platinum SuperFi RT-PCR Master Mix, 0.25 μL SuperScript IV RT Mix, for primer amount optimization, 1-3 μL of 10 μM forward primer, and 1-3 μL of 10 μM reverse primer is mixed with 5 uL isolated RNA for a total RT-PCR volume of 25 μL. RT-PCR thermocycler program set at 55°C for 10 minutes to allow cDNA synthesis then subjected to a standard PCR protocol (denaturation [5 minutes at 98°C], amplification [42 cycles: 10 seconds at 98°C, 10 seconds at 59°C, 15 seconds at 72°C], and elongation [5 minutes at 72°C]). Gradient temperatures from 55°C to 68°C was used for annealing temperature optimizations. For RT-RPA, RPA pellets were resuspended in 29.5 μL of the supplied Rehydration Buffer, and 11.8 μL of this RPA solution, 3 μL of forward primer (10 μM), 3 μL of reverse primer (10 μM), 3.2 μL of nuclease-free water, 4 μL of MgOAC (280 mM), and 5 μL isolated RNA sample were mixed and incubated at 42°C for 20 min. Primer sequences are listed in Table S1 and were purchased from Integrated DNA Technologies (IDT).

CRISPR detection assay

For CRISPR detection, 2 μL of RT-PCR product is put into a 96 well Corning Half Area Opaque well and mixed with 30 uL of CRISPR mix composed of: 3 μL NEBuffer 2.1, 0.01 μL 100 μM gRNA, 0.02 to 0.06 μL 100 μM EnGen Lba Cas12a, 1 to 3 μL of 10 μM fluorescent probe, and 25.47 μL nuclease-free water. Plate incubated for 20 mins at 37°C in the dark, and fluorescent read by SpectraMax i3x Multi-Mode Microplate Reader (Molecular Devices) excited at 495 nm and 535 nm. For probe concentration optimization, CRISPR reaction contained ratios of 1:15, 1:20, and 1:25 of Cas12a/gRNA to probe concentration incubated at 37°C. For temperature optimization, a Cas12a/gRNA to probe concentration of 1:15 is used with incubation temperatures of 27°C, 37°C, and 42°C. Thresholds for positive CRISPR signal were independently defined as the mean plus three times the SD of the negative template control sample

or negative sample for assays performed with RNA isolated from viral cultures or clinical specimens, respectively, since these RNA samples were isolated with different RNA extraction kits and yielded different background fluorescence values. Sequences for the fluorescent probe and Cas12a gRNAs are listed in Table S1 and were purchased from IDT.

Standard curve and limit of detection (LoD)

Standard curve and LoD assays were performed by spiking known concentrations of SARS-CoV-2 RNA into healthy donor nasal swab samples and serially diluting this solution with healthy human nasal swab samples. Dilutions created, in copies/μL, were 0.5, 1, 5, 10, 50, 100, 500, and 1,000. RNA was extracted from each of these dilution samples for amplification and CRISPR detection assay steps.

Cellphone detection for quantitative point-of-care readout

Cellphone device designed in AutoDesk inventor and 3D-printed by StraSys uPrint SE Plus. A 3D-printed device designed to fit Samsung Galaxy S9 with 12.2-megapixel, 7.06-mm CMOS image sensor and rear camera with 26-mm focal length. Powered by three AAA batteries, fluorescent is excited by blue laser diode (465 nm, >100 mW, DTR's Laser Shop) connected to heatsink mounted to the base of 3D-printed device. Convex lens (f_2 = 50 mm, Edmund Optics, #38-296) place in device for signal collection with a demagnification index calculated as $M = f_1/f_2 \approx 0.52$, and a 525-nm band-pass filter (Edmund Optics, #86-354) that was placed in front of the smartphone camera as an emission. For the on-chip CRISPR-FDS assays, 10 μL of an RT-RPA CRISPR solution generated by mixing equal volumes of the RT-RPA and CRISPR-FDS reaction mixtures was pre-loaded into each chip well, after which 5 μL of saliva lysate or purified RNA was loaded into these wells, and the chip was incubated at $\geq$22°C for 5 min.

QUANTIFICATION AND STATISTICAL ANALYSIS

CRISPR assay signal expressed as the mean of ±SD from 3 independent reactions. GraphPad Prism 8 was used to create ROC curves to determine cutoff values for targets D614G, D950N, and S982A. Differences considered statistically significant at $P < 0.05$. Cutoff values for Figures 1 and 2 vs. Figures 3 and 4 are different because the sample types (viral seed stocks and nasal swab samples, respectively) are different and RNA was extracted using different kits, which both cause changes in background signal and therefore the cutoff values. Statistical details can be found in the results and figure legends.